Vibrational relaxation of the $2A_g^-$ excited state in all-*trans*-β-carotene obtained by femtosecond time-resolved Raman spectroscopy

M. Yoshizawa and H. Aoki

Department of Physics, Graduate School of Science, Tohoku University, Aramaki-aza-aoba, Aoba-ku, Sendai 980-8578, Japan

H. Hashimoto

Department of Materials Science and Chemical Engineering, Faculty of Engineering, Shizuoka University, Johoku, Hamamatsu 432-8561, Japan

Relaxation kinetics in all-*trans*-β-carotene has been investigated by recently developed femtosecond Raman spectroscopy. We observed the stimulated Raman signal of the $2A_g^-$ excited state which is converted from the photogenerated $1B_u^+$ state. The vibrational relaxation in the $2A_g^-$ state takes place within 0.6 ps until the $l = 1$ vibrational level, but the relaxation from the $l=1$ level to the $l=0$ level is slower than 10 ps. The unusual kinetics is explained in terms of the $1B_u^-$ state which exists between the $l=1$ and $l=2$ levels of the $2A_g^-$ state.

All-*trans*-carotenoids play an important role in the light-harvesting function in bacterial photosynthesis.[1,2] The linear polyene structure has been also attracted much interest in relation to conjugated polymers. The ground state of the carotenoid has the $1A_g^-$ symmetry assuming the C_{2h} symmetry of its polyene backbone. Therefore, the lowest singlet excited state, $2A_g^-$, is optically forbidden. The lowest optically active state is the $1B_u^+$ state. Recently, another dark state, $1B_u^-$, has been predicted and discovered between the $1B_u^+$ and $2A_g^-$ states.[3,4] The relaxation kinetics in the carotenoids has been intensively investigated using time-resolved spectroscopy.[5–13] The photogenerated $1B_u^+$ state converts to the $2A_g^-$ state within 100–300 fs and the lifetime of the $2A_g^-$ state is several picoseconds. In the case of carotenoids in the light-harvesting complexes, the lifetime becomes shorter due to the ultrafast energy transfer reactions from carotenoids to bacteriochlorophyll.[6,7]

It has been generally considered that the vibrational relaxation time of electronic excited states in large molecules is shorter than 1 ps.[14] Actually, the vibrational relaxation of the $1B_u^+$ state in all-*trans*-β-carotene (β-carotene) has been found to be shorter than 100 fs by femtosecond fluorescence spectroscopy.[8,9] The subpicosecond spectral change observed by femtosecond absorption spectroscopy has been explained by the vibrational relaxation of the $2A_g^-$ state.[10] However, Zhang *et al.* have recently reported that the vibrational relaxation of the $2A_g^-$ state in all-*trans*-lycopene is slower than the internal conversion to the ground state.[11] The energy transfer in the photosynthesis has been assumed to occur from the lowest vibrational level of the excited states, but the theoretical calculation using the assumption cannot explain the ultrafast transfer rate.[15] Therefore, the vibrational relaxation kinetics in carotenoids is very important to understand the mechanism of the highly efficient energy transfer in photosynthesis.

The vibrational relaxation of the optically forbidden $2A_g^-$ state has been investigated using time-resolved absorption spectroscopy.[10,11] However, it is difficult to assign the 0-0 transition and the vibrational modes, because the absorbance change contains absorption of the transient states, bleaching of the ground state, and stimulated emission from the excited states. The sub-10 fs time-resolved study has observed the oscillation of the ground state after the photoexcitation, but the oscillation of the $2A_g^-$ state cannot be observed because of the dephasing in the internal conversion.[13] The time-resolved Raman signals in β-carotene have been already observed by picosecond Raman spectroscopy.[12,16,17] The $C = C$ stretching mode of the $1A_g^-$ ground state at 1521 cm^{-1} decreases by the photoexcitation and the same mode of the $2A_g^-$ state appears at 1777 cm^{-1}. The abnormally high frequency in the $2A_g^-$ state has been explained in terms of the vibronic coupling between the $2A_g^-$ and $1A_g^-$ states through the totally symmetric $C = C$ stretching vibration. However, the temporal dependence of the Raman signal has not been time resolved, because the ordinary Raman spectroscopy cannot have the femtosecond temporal resolution with sufficient spectral resolution.

Here, we present a study of the photoexcited states in β-carotene using femtosecond time-resolved Raman spectroscopy. The photoinduced absorbance change has been also measured and compared with the Raman signals. The internal conversion from the photogenerated $1B_u^+$ state to the $2A_g^-$ state and the vibrational relaxation of the $2A_g^-$ state are discussed.

The experimental setup of the femtosecond time-resolved Raman spectroscopy was described in detail elsewhere.[18] Briefly, the 100 fs seed pulse generated by a mode-locked Ti:sapphire laser (Avesta) was amplified by a kHz regenerative amplifier (Spectra Physics). The amplified pulse was separated to three beams. The second harmonic pulse (397 nm, 150 fs) of the first beam was used as the first pump pulse for the generation of the photoexcited states. The second beam passed through an interference filter [794 nm, full width at half maximum (FWHM) 23 cm^{-1}] and was used as the Raman pump pulse. The femtosecond supercontinuum pulse generated from the last beam was used as the probe pulse. The Raman signal of the excited states was observed as the transmittance change due to the stimulated Raman scattering induced by the Raman pump pulse. The temporal resolution of the equipment was determined to be 300 fs by the correlation between the first pump and probe pulses. The spectral resolution was determined to be 25 cm^{-1} by the

63 180301-1
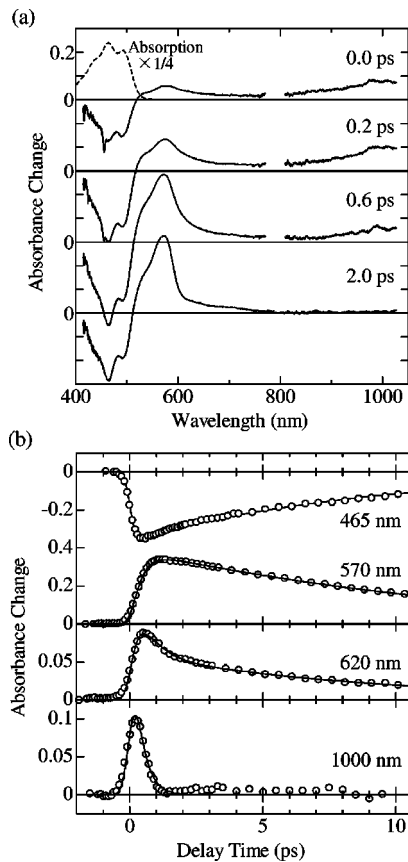
FIG. 1. (a) Time-resolved absorbance change spectra induced by the 397 nm pump pulse, and (b) transient absorbance changes at selected probe wavelengths. The solid lines are the best fits to the data.

FIG. 2. (a) Time-resolved Raman spectra on the anti-Stokes side, and (b) time profiles of the Raman signal. The Raman loss signal appears positive. Hatched signals are due to the solvent, benzene.

bandwidth of the Raman pump pulse and the resolution of the spectrometer. The polarizations of the pulses were parallel to one another.

All-*trans*-β-carotene was purchased from Wako Pure Chemical Industries Ltd., and recrystallized twice from benzene. Concentrations in the benzene solution for the femtosecond absorption and Raman measurements were 8×10^{-5} M and 4×10^{-4} M, respectively. The solution was circulated using a 1 mm flow cell. The photon densities of the first pump pulse were 4×10^{15} and 2×10^{16} photons/cm^2 for the absorption and Raman measurements, respectively. The photon density of the Raman pump pulse was 6×10^{16} photons/cm^2. The measurements were performed at room temperature.

The time-resolved absorbance changes after the 397 nm photoexcitation are shown in Fig. 1. A sharp negative signal at 455 nm is observed at a delay time of 0.0 ps. It is assigned to the Raman gain of C-H stretching modes in β-carotene and benzene. The absorbance changes of β-carotene have three structures, bleaching at 400–500 nm, absorption at 500–700 nm, and absorption around 1000 nm. The temporal responses of the absorbance changes are shown in Fig. 1(b). The solid curves are the best fitted curves using exponential rise and decay components with convolution of the resolution time. The absorption at 1000 nm appears instantaneously after the photoexcitation and disappears with a life-

time of 0.35 ± 0.05 ps. The bleaching at 465 nm appears instantaneously and disappears with a lifetime of 8.8 ± 0.2 ps. The temporal responses with the time constants of 0.35 and 8.8 ps are also observed around 570 nm as a fast rise component and a slow decay component, respectively. The 620 nm absorption has the other fast decay component with the time constant of 0.53 ± 0.1 ps. On the other hand, the absorption at 570 nm has the other slow rise component with the time constant of a few picoseconds. Therefore, the absorption peak at 570 nm becomes sharp at 2.0 ps.

Since the lifetime of the absorption at 1000 nm is nearly equal to the lifetime of the fluorescence,[8,9] it is assigned to the transition from the photogenerated $1B_u^+$ state to higher excited states. The absorption around 570 nm is assigned to the transition from the $2A_g^-$ state, because the rise time is consistent with the decay time of the $1B_u^+$ state and the lifetime is equal to the recovery time of the bleaching. The initial spectral change around 570 nm has been also observed in other carotenoids.[10,11] It is assigned to the vibrational relaxation of the $2A_g^-$ state.

The time-resolved Raman signals after the 397 nm photoexcitation are shown in Fig. 2. The absorbance change induced by the Raman pump pulse was measured on the anti-Stokes side around 700 nm (inverse Raman signal). The Raman signal is separated from the extra broad signal which is induced by the resonant excitation. Since the intensity of the Raman pump pulse decreases by the absorption of the excited states, the Raman signal at each delay time is normalized using a Raman line in benzene at 991 cm^{-1}.
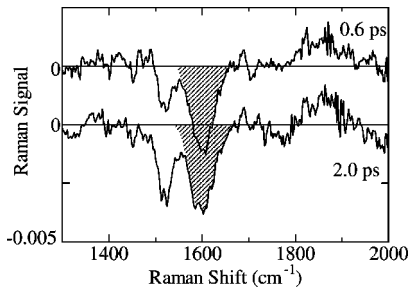
FIG. 3. Time-resolved Raman spectra on the Stokes side. The Raman gain signal appears negative.

The signal at delay time of -5 ps gives the Raman signal of the $1A_g^-$ ground state in β-carotene. A peak at 1520 cm^{-1} is assigned to the $C=C$ stretching mode. The other peak at 1590 cm^{-1} is due to benzene. After the 397 nm photoexcitation, the 1520 cm^{-1} peak decreases instantaneously and the signal due to the transient states appears around 1790 cm^{-1}. The Raman shift of the new signal is almost equal to that of the $C=C$ stretching mode of the $2A_g^-$ state observed by the picosecond studies.[12,16,17] However, the spectral and temporal features are remarkably interesting. The negative signal at 0.2 ps has a peak at 1770 cm^{-1}, but it becomes broad and shifts to 1790 cm^{-1} at 0.6 ps. At 2.0 ps, the signal has a dispersive shape which has a positive peak at 1750 cm^{-1} and a negative peak at 1810 cm^{-1}. The Raman signals on the Stokes side are just the inverse of the signals on the anti-Stokes side as shown in Fig. 3. The dispersive structure is also observed on the Stokes side around 1790 cm^{-1}. At the longer delay times, the signal becomes smaller without changing the dispersive shape.

The negative and dispersive Raman signals are unusual, so the origins should be carefully discussed. The delay time dependence on the 397 nm pump pulse shows that the signals are due to the photoexcited states. The delay time dependence on the Raman pump pulse follows the temporal profile of the pulse. Therefore, the signals are due to the coherent process induced by the Raman pump pulse or due to a higher excited state with an ultrashort lifetime which is highly excited by the Raman pump pulse. The stimulated emission from the higher excited state can give the negative signal. However, the Raman shift of each signal is not affected by the change of the Raman pump wavelength. The observed signals are concluded to be due to the stimulated Raman scattering.

The Raman process is usually discussed on an assumption that a vibrational ground level is the initial state. The stimulated Raman signal on the anti-Stokes side is positive in the case of off-resonant Raman pump and probe pulses (Raman loss), while the dispersive Raman signal has been observed in the case of a near-resonant probe pulse.[19] However, the probe pulse used in this study was off resonance from the transient absorption peak at 570 nm. Moreover, the signal on the Stokes side is always negative (Raman gain) and cannot have the dispersive shape even in the near-resonant case. The dispersive signals observed on both the anti-Stokes and Stokes sides cannot be explained by the resonance.

Since the photoexcited state remains in the vibrational excited levels in the femtosecond region, the effect must be considered. The change of the vibrational quantum number in the Raman process is usually positive ($\Delta l = +1$), because the vibrational ground level is the initial state. When the vibrational excited level is the initial state, the negative change ($\Delta l = -1$) is available and the signal on the anti-Stokes side becomes negative. The absorbance change due to the stimulated Raman process between two vibrational levels, $l = j$ and $l = j + 1$ ($j = 0, 1, 2, \ldots$), can be represented using a Lorentzian function as

$$\Delta A(\Delta\omega) \propto \pm \frac{n_j - n_{j+1}}{(\Delta\omega - \omega_v)^2 + \gamma_v^2}, \qquad (1)$$

where $\Delta\omega$ is the Raman shift, n_j and n_{j+1} are the populations in the respective vibrational levels, and ω_v and γ_v are the frequency and the relaxation rate of the transition, respectively. The plus and minus signs correspond to the signals on the anti-Stokes and Stokes sides, respectively.

The dispersive signal around 1790 cm^{-1} can be simulated using two Lorentzian curves centered at 1770 and 1800 cm^{-1} with a common bandwidth of 120 cm^{-1}. Figure 2(b) shows the temporal dependence of the signals. The 1770 cm^{-1} component appears as the negative signal with a time constant of 0.35 ps. It increases with a time constant of 0.6 ps and becomes positive. The negative 1800 cm^{-1} component appears with a time constant of 0.6 ps. The decay kinetics of both components can be represented by the 8.8 ps lifetime. Therefore, both of the 1770 and 1800 cm^{-1} components are assigned to the $2A_g^-$ state. The transient change of the sign at 1770 cm^{-1} is explained by the vibrational relaxation from the upper level to the lower level. Just after the photoexcitation, the larger population in the upper level gives the negative signal. Then, the population of the lower level becomes larger with the vibrational relaxation and the signal becomes positive. The long-lived negative signal at 1800 cm^{-1} means that the $2A_g^-$ state remains in the vibrational excited level longer than several picoseconds. It is assigned to the first vibrational excited level ($l = 1$) of the $2A_g^-$ state. The 0.6 ps relaxation is assigned to the vibrational relaxation from the higher excited levels ($l \geqslant 2$) to the $l = 1$ level.

The stimulated Raman signal and photoinduced absorbance change have not changed the spectral features at the delay times longer than 2.0 ps. These results mean that the vibrational relaxation from the $l = 1$ level is slower than the internal conversion to the ground state. The fast and slow vibrational relaxations of the $2A_g^-$ state can be explained in terms of the $1B_u^-$ state. Since the $1B_u^-$ state in the crystalline β-carotene is 1880 cm^{-1} above the $2A_g^-$ state,[4] it is expected to exist between the $l = 1$ and $l = 2$ levels of the $2A_g^-$ state. The ultrafast vibrational relaxation until the $l = 1$ level is considered to be assisted by the $1B_u^-$ state.

The 1520 cm^{-1} signal due to the $1A_g^-$ ground state decreases instantaneously with the photoexcitation. The recovery time is longer than the lifetime of the bleaching, 15 ± 3 ps. It is explained by the vibrational relaxation of the ground state after the internal conversion from the $2A_g^-$ state to hot vibrational levels of the ground state.
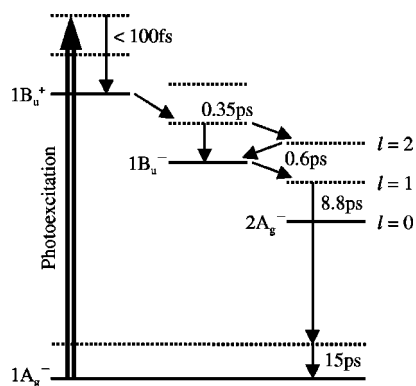
FIG. 4. Schematic energy diagram of all-*trans*-β-carotene and relaxation kinetics after photoexcitation. The numbers in the $2A_g^-$ state denote the vibrational levels.

The relaxation kinetics in β-carotene is expressed using the energy diagram shown in Fig. 4. First, the 397 nm pump pulse generates the vibrational excited levels of the $1B_u^+$ state. Since the vibrational relaxation (redistribution) of the $1B_u^+$ state is very fast,[8,9] the initial photogenerated state observed in this study is the lowest vibrational level of the $1B_u^+$ state. The $1B_u^+$ state converts to the $2A_g^-$ state through the $1B_u^-$ state with the time constant of 0.35 ps. The highly vibrational excited level ($l=2$) of the $2A_g^-$ state is generated at this time scale. The negative Raman signal at 1770 cm^{-1} is assigned to the transition from the $l=2$ level to the $l=1$ level. Then, the vibrational relaxation from the $l=2$ level to the $l=1$ level takes place with the time constant of 0.6 ps. The 1770 cm^{-1} signal changes to positive ($l=1\rightarrow l=2$) and the negative 1800 cm^{-1} signal ($l=1\rightarrow l=0$) appears. The fast decay component of the absorption at 620 nm is explained by this relaxation. Therefore, the absorption peak at 570 nm is assigned to the transition from the $l=1$ level of the $2A_g^-$ state to a higher excited state. Finally, the internal conversion to the $1A_g^-$ ground state takes place with the lifetime of 8.8 ps followed by the vibrational relaxation of the ground state.

The difference of the Raman shifts between the $l=1\leftrightarrow l=2$ and $l=0\leftrightarrow l=1$ transitions can be explained by the vibrational coupling. The vibrational excited levels of the $2A_g^-$ and $1A_g^-$ states in carotenoids are coupled through the $C=C$ stretching vibrational mode.[16,17] The coupling pushes down the $l=1$ level of the $1A_g^-$ ground state and pushes up the $l=1$ level of the $2A_g^-$ state. The shift of the $l=2$ level of the $2A_g^-$ state is expected to be smaller than the $l=1$ level, because the coupling between higher excited levels is generally smaller. Therefore, the frequency of the $l=1\leftrightarrow l=2$ transition is smaller than that of the $l=0\leftrightarrow l=1$ transition.

The contradictory results observed in other carotenoids can be explained by the difference of the energy levels. The slow and small spectral change observed in lycopene[11] is assigned to the slow vibrational relaxation from the $l=1$ level, because of its similar energy levels with β-carotene.[4] The fast and large spectral changes observed in the long carotenoids[10] are probably due to the vibrational relaxation to the $l=0$ level of the $2A_g^-$ state. Since the separations of the energy levels become smaller in longer carotenoids, the $1B_u^-$ state in the long carotenoids is expected to become lower than the $l=1$ level of the $2A_g^-$ state. Therefore, the $1B_u^-$ state can assist the vibrational relaxation to the $l=0$ level.

In conclusion, the Raman signal of the $2A_g^-$ excited state in all-*trans*-β-carotene has been time resolved. The negative stimulated Raman signal on the anti-Stokes side indicates that the vibrational excited levels of the $2A_g^-$ state are generated after the photoexcitation. The vibrational relaxation of the $2A_g^-$ state is very fast until the $l=1$ level, but that from the $l=1$ level is slower than the internal conversion to the ground state. The vibrational excited levels should be considered on the energy transfer in the photosynthesis.

[1] Y. Koyama, M. Kuki, P. O. Andersson, and T. Gillbro, Photochem. Photobiol. **63**, 243 (1996).

[2] H. A. Frank and R. J. Cogdell, Photochem. Photobiol. **63**, 257 (1996).

[3] P. Tavan and K. Shulten, Phys. Rev. B **36**, 4337 (1987).

[4] T. Sahima, Y. Koyama, T. Yamada, and H. Hashimoto, J. Phys. Chem. **B104**, 5011 (2000).

[5] A. P. Shreve, J. K. Trautman, T. G. Owens, and A. C. Albrecht, Chem. Phys. Lett. **178**, 89 (1991).

[6] M. Ricci, S. P. Bradforth, R. Jimenez, and G. R. Fleming, Chem. Phys. Lett. **259**, 381 (1996).

[7] J.-P. Zhang, R. Fujii, P. Qian, T. Inaba, T. Mizoguchi, Y. Koyama, K. Onaka, Y. Watanaba, and H. Nagae, J. Phys. Chem. B **104**, 3683 (2000).

[8] H. Kandori, H. Sasabe, and M. Mimuro, J. Am. Chem. Soc. **116**, 2671 (1994).

[9] S. Akimoto, I. Yamazaki, S. Takeuchi, and M. Mimuro, Chem. Phys. Lett. **313**, 63 (1999).

[10] P.O. Andersson and T. Gillbro, J. Chem. Phys. **103**, 2509 (1995).

[11] J.-P. Zhang, C-H. Chen, Y. Koyama, and H. Nagae, J. Phys. Chem. B **102**, 1632 (1998).

[12] H. Nagae, M. Kuki, J.-P. Zhang, T. Sashima, Y. Kumai, and Y. Koyama, J. Phys. Chem. A **104**, 4155 (2000).

[13] G. Lanzani, G. Cerullo, M. Zavelani-Rossi, and S. De Silvestri, Synth. Met. **116**, 1 (2001).

[14] T. Elsaesser and W. Kaiser, Annu. Rev. Phys. Chem. **42**, 83 (1991).

[15] A. Damjanovic, T. Ritz, and K. Schulten, Phys. Rev. E **59**, 3293 (1999).

[16] H. Hashimoto and Y. Koyama, Chem. Phys. Lett. **163**, 251 (1989).

[17] T. Noguchi, S. Kolaczkowski, C. Arbour, S. Aramaki, G. H. Atkinson, H. Hayashi, and M. Tasumi, Photochem. Photobiol. **50**, 603 (1989).

[18] M. Yoshizawa and M. Kurosawa, Phys. Rev. A **61**, 013808 (2000).

[19] S. Saikan, N. Hashimoto, T. Kushida, and K. Namba, J. Chem. Phys. **82**, 5409 (1995).